

Mesoscale simulation model for odd fluids

Yuxing Jiao* and Mingcheng Yang†

*Beijing National Laboratory for Condensed Matter Physics and Laboratory of Soft Matter Physics,
Institute of Physics, Chinese Academy of Sciences, Beijing 100190, China and
School of Physical Sciences, University of Chinese Academy of Sciences, Beijing 100049, China*

A fluid, with broken time-reversal symmetry, would exhibit odd transport coefficients, such as odd viscosity, thermal conductivity and diffusion coefficient, which may fundamentally alter the fluid properties and significantly influence the structure and dynamics of immersed objects. Here, we develop an efficient coarse-grained simulation approach for the odd fluid, that captures all essential features of real odd fluids. Based on microscopic kinetic theory, we analytically derive the transport coefficients of the mesoscale odd fluid. Furthermore, we validate our approach by performing both simulations and theoretical calculations to explore the intricate transport phenomena of the odd fluid under various external drivings. Our work thus paves the way for studying anomalous transport in odd fluids and for large-scale simulations of odd complex fluids.

Introduction.—In common fluids, transport coefficient tensor, that relates fluxes to drivings, is symmetric (even) under time reversal, which is required by Onsager reciprocal relations [1]. However, when time-reversal and parity symmetries of a fluid are broken, its transport coefficient tensor is predicted to contain additional anti-symmetric part that are odd under time reversal. The odd transport coefficients have been extensively studied across many scales, such as the appearance of odd viscosity in electron Hall fluids [2–5], odd viscosity and thermal conductivity in polyatomic gases under a magnetic field [6, 7], odd diffusivity in charged particles in a magnetic field [8–10], and odd viscosity and diffusivity in chiral active fluids [11–18]. The odd transport coefficients can produce transverse fluxes under longitudinal drivings and give rise to many intriguing phenomena unattainable in common fluids [12, 13, 19–25].

Besides fundamentally changing the properties of the fluid itself, the odd transport coefficients are expected to importantly influence the structure and dynamics of mesoscopic objects immersed in the fluid. However, the study on such odd complex fluids (composed of mesoscopic objects in odd fluids) is rare and nontrivial, because of its many-body character and the complex interplay between diverse interactions. Even a few existing numerical works [17, 19, 21, 24, 26], based on molecular-dynamics-type simulations, mainly focus on a single suspending object, due to the computational bottleneck arising from the drastic difference in time and length scales between solvent and solute particles. In contrast, several coarse-grained fluid approaches have been well established to simulate traditional complex fluids during the past few decades, e.g., lattice Boltzmann method [27–29], dissipative particle dynamics [30, 31] and multi-particle collision dynamics (MPC) [32–36]. The coarse-grained approaches extremely speed up the simulations of traditional complex fluids and have achieved considerable success. Hence, it is highly desired to develop an efficient coarse-grained model for the odd fluid, that is critical for exploring the emerging odd complex fluids.

In this Letter, by slightly generalizing the widely-used version of MPC, i.e., stochastic rotation dynamics (SRD), we propose a coarse-grained odd fluid model, named chiral stochastic rotation dynamics (CSR D), that has all odd transport coefficients (odd viscosity, thermal conductivity and diffusion coefficient). The CSR D method retains all the advantages of the conventional SRD, such as high efficiency, proper description of hydrodynamics, dissipation, thermal fluctuations, and so on. Furthermore, the simplicity of the CSR D enables us to derive analytical expressions for its odd transport coefficients, which agree precisely with simulation measurements. By means of both simulations and continuum theory, we show that the CSR D exhibits significant transverse fluxes under various external drivings and correctly capture the intriguing transport behavior of odd fluids.

The CSR D Model.—Following the conventional SRD, the CSR D fluid is described with a large number of point particles of mass m with continuous positions $\mathbf{r}_i(t)$ and velocities $\mathbf{v}_i(t)$. For simplicity, we here consider a two-dimensional isotropic CSR D fluid, which can be straightforwardly extended to three dimensions. The dynamics of the mesoscopic fluid consists of alternating streaming and collision steps. In the streaming step, each fluid particle (say i) moves ballistically for a certain time Δt ,

$$\mathbf{r}_i(t + \Delta t) = \mathbf{r}_i(t) + \mathbf{v}_i(t)\Delta t. \quad (1)$$

In the collision step, the particles are sorted into cells of a square lattice with a size l , and then their velocities relative to the center-of-mass velocity of each cell are rotated around the z axis by an angle α

$$\mathbf{v}_i(t + \Delta t) = \mathbf{v}_{cm} + \mathbf{R}(\alpha) \cdot (\mathbf{v}_i(t) - \mathbf{v}_{cm}), \quad (2)$$

with \mathbf{v}_{cm} the center-of-mass velocity of the collision cell and $\mathbf{R}(\alpha)$ the rotation matrix. To ensure Galilean invariance, the lattice's position is randomly shifted for each collision step [37]. For the conventional SRD, the rotational angle is $\alpha = \Omega$, where Ω is randomly taken as ω or $-\omega$ with equal probability (independently for each cell);

while, for the CSRD, $\alpha = \Omega + \theta$, where an additional unidirectional rotation with a fixed angle θ is implemented. When $\theta = 0$, the CSRD trivially reduces to the SRD. It is just the additional unidirectional rotation that breaks the time-reversal and parity symmetries, thus allowing the presence of odd transport coefficients that are lacking in the conventional SRD. The effect of the nonzero θ is reminiscent of the role played by a constant external magnetic field in charged particle systems.

Except for allowing the presence of odd transport coefficients, the CSRD fluid retains all other features of the common SRD fluid, which is crucial to properly capture hydrodynamic behavior. For instance, the CSRD locally conserves mass, momentum and energy, and obeys the H-theorem as confirmed in Fig. 1(a), in which the H-function, $H(t) = \int d\mathbf{v} f(\mathbf{v}, t) \ln f(\mathbf{v}, t)$ with $f(\mathbf{v}, t)$ the single-particle velocity distribution, decreases rapidly with time and converges to a steady-state value. Without external perturbation, the CSRD quickly evolves into equilibrium state with a Maxwellian velocity distribution, as shown in Fig. 1(b). Moreover, the CSRD fluid satisfies an ideal gas equation of state owing to the absence of potential interaction (Fig. 1(c)).

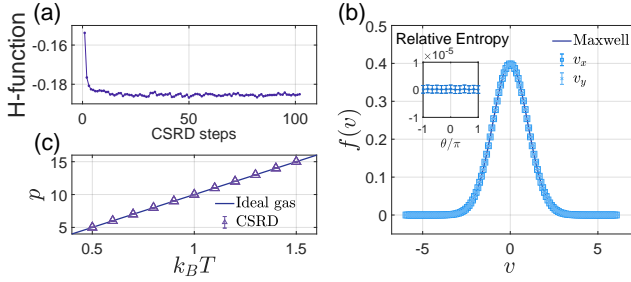


FIG. 1. (a) The evolution of H-function in the CSRD simulation. (b) The single-particle velocity distribution, where the symbols and curve correspond to the simulation data and the standard Maxwellian distribution, respectively. The inset is the vanishing KL-divergence at different θ : $D_{KL}(f(\mathbf{v})||f_{Eq}(\mathbf{v})) = \int d\mathbf{v} f(\mathbf{v}) \ln [f(\mathbf{v})/f_{Eq}(\mathbf{v})]$, which measures the difference between the joint velocity distribution and its equilibrium counterpart. (c) Pressure as a function of temperature with a fixed particle number density n . The triangles represent the simulation results for 5 different θ ($0, \pi/4, \pi/2, 3\pi/4, \pi$), which coincide together and agree perfectly with the ideal gas equation of state (solid line). In (a-c), $\omega = 2\pi/3$, $n = 10$ and $\Delta t = 0.1$; and in (a,b) $k_B T = 1$ and $\theta = 5\pi/9$. In simulations, all quantities are nondimensionalized by setting $m = 1$, $l = 1$ and the mean thermal energy = 1.

Hydrodynamic theory and transport coefficients.—The CSRD model properly describe the hydrodynamics of real odd fluids. The hydrodynamic equations can be derived via a microscopic kinetic theory [38] originally developed by Pooley and Yeomans for determining the

transport coefficients of the conventional SRD. In this approach, the system is approximated to be in local equilibrium, with the single-particle distribution being a function of local thermodynamic variables. According to the CSRD dynamics (Eqs. (1)-(2)), the fluxes of conserved quantities, including mass, momentum and energy, are directly derived through lengthy calculations (see Supplementary Material [39] for the detailed derivation). Note that both streaming and collision steps may contribute to the fluxes of the conserved quantities. The transport coefficients can be extracted from the expressions of these fluxes. And, substituting the fluxes into the corresponding conservation equations separately yields the mass continuity equation, the Navier-Stokes equation and the heat conduction equation,

$$\begin{aligned} \partial_t \rho + \partial_\alpha (\rho u_\alpha) &= 0, \\ \partial_t (\rho u_\alpha) + \partial_\beta (\rho u_\alpha u_\beta) &= \partial_\beta \sigma_{\alpha\beta}, \\ \frac{k_B}{m} [\partial_t (\rho T) + \partial_\alpha (\rho T u_\alpha)] &= \sigma_{\alpha\beta} \partial_\beta u_\alpha + \partial_\alpha (\kappa_{\alpha\beta} \partial_\beta T), \end{aligned} \quad (3)$$

with $\rho = mn(\mathbf{r}, t)$ the local mass density, $\mathbf{u}(\mathbf{r}, t)$ the local fluid velocity, and $T(\mathbf{r}, t)$ the local temperature. Here, the stress tensor $\sigma_{\alpha\beta}$ and the thermal conductivity tensor $\kappa_{\alpha\beta}$ take the following forms:

$$\begin{aligned} \sigma_{\alpha\beta} &= -p\delta_{\alpha\beta} + [\eta (\delta_{\alpha\mu}\delta_{\beta\nu} + \delta_{\alpha\nu}\delta_{\beta\mu} - \delta_{\alpha\beta}\delta_{\mu\nu}) \\ &\quad + \zeta\delta_{\alpha\beta}\delta_{\mu\nu} + \eta_R (\delta_{\alpha\mu}\delta_{\beta\nu} - \delta_{\alpha\nu}\delta_{\beta\mu}) \\ &\quad + \eta_o (\varepsilon_{\alpha\mu}\delta_{\beta\nu} + \varepsilon_{\beta\nu}\delta_{\alpha\mu}) \\ &\quad - \eta_A \varepsilon_{\alpha\beta}\delta_{\mu\nu} - \eta_B \delta_{\alpha\beta}\varepsilon_{\mu\nu}] \partial_\nu u_\mu, \\ \kappa_{\alpha\beta} &= \kappa\delta_{\alpha\beta} + \kappa_o \varepsilon_{\alpha\beta}, \end{aligned} \quad (4)$$

with $\delta_{\alpha\beta}$ the Kronecker delta, $\varepsilon_{\alpha\beta}$ the Levi-Civita tensors and p the pressure.

In the stress tensor of Eqs. (4), η refers to the shear viscosity, ζ to the bulk viscosity, η_R to the rotation-rotation viscosity, η_o to the odd viscosity, η_A to the compression-rotation viscosity, and η_B to the rotation-compression viscosity. Their physical meanings can be clearly found for instance in reference [13]. Therein, η , ζ and η_R are even with respect to θ , while η_o , η_A and η_B are odd. In addition, the thermal conductivity tensor also contains an even component κ and an odd component κ_o . With the contributions separately from the streaming/kinetic (*kin*) and collision (*col*) steps, the coefficients above become,

$$\begin{aligned} \eta &= \eta^{kin} + \frac{1}{2}\eta^{col}, & \zeta &= \frac{1}{2}\eta^{col}, & \eta_R &= \frac{1}{2}\eta^{col} \\ \eta_o &= \eta_o^{kin} + \frac{1}{2}\eta_o^{col}, & \eta_A &= -\frac{1}{2}\eta_o^{col}, & \eta_B &= \frac{1}{2}\eta_o^{col} \\ \kappa &= \kappa^{kin} + \kappa^{col}, & \kappa_o &= \kappa_o^{kin} + \kappa_o^{col}. \end{aligned} \quad (5)$$

Here, the kinetic and collisional contributions are analytically calculated as,

$$\eta^{kin} = nk_B T \Delta t \left[\frac{\lambda}{\lambda - 1 + e^{-\lambda}} \frac{1 - \cos 2\theta \cos 2\omega}{1 + \cos 2\omega (\cos 2\omega - 2 \cos 2\theta)} - \frac{1}{2} \right], \quad (6a)$$

$$\eta^{col} = \frac{m}{12\Delta t} (\lambda - 1 + e^{-\lambda}) (1 - \cos \theta \cos \omega), \quad (6b)$$

$$\eta_o^{kin} = -nk_B T \Delta t \frac{\lambda}{\lambda - 1 + e^{-\lambda}} \frac{\sin 2\theta \cos 2\omega}{1 + \cos 2\omega (\cos 2\omega - 2 \cos 2\theta)}, \quad (6c)$$

$$\eta_o^{col} = \frac{m}{12\Delta t} (\lambda - 1 + e^{-\lambda}) \sin \theta \cos \omega, \quad (6d)$$

$$\kappa^{kin} = n \frac{k_B^2 T}{m} \Delta t \left\{ \frac{\lambda \left[(\lambda + 2 \cos \omega) \sin^2 \frac{\omega}{2} + ((\lambda - 2) \cos \omega + 4 \cos 2\omega \cos^2 \frac{\theta}{2}) \sin^2 \frac{\theta}{2} \right]}{(\lambda - 1) \left\{ (\lambda + 2 \cos \omega)^2 \sin^4 \frac{\omega}{2} + [(\lambda - 2) (\lambda - 1 - \cos 2\omega) \cos \omega + 4 (\lambda - 1) \cos 2\omega \cos^2 \frac{\theta}{2}] \sin^2 \frac{\theta}{2} \right\}} - 1 \right\}, \quad (6e)$$

$$\kappa^{col} = \frac{k_B (\lambda - 1)}{6\lambda \Delta t} (1 - \cos \theta \cos \omega), \quad (6f)$$

$$\kappa_o^{kin} = -n \frac{k_B^2 T}{m} \Delta t \frac{\lambda^2 [(\lambda - 2) \cos \omega + 2 \cos 2\omega \cos \theta] \sin \theta}{2 (\lambda - 1) \left\{ (\lambda + 2 \cos \omega)^2 \sin^4 \frac{\omega}{2} + [(\lambda - 2) (\lambda - 1 - \cos 2\omega) \cos \omega + 4 (\lambda - 1) \cos 2\omega \cos^2 \frac{\theta}{2}] \sin^2 \frac{\theta}{2} \right\}}, \quad (6g)$$

$$\kappa_o^{col} = \frac{k_B (\lambda - 1)}{6\lambda^2 \Delta t} \sin \theta \cos \omega, \quad (6h)$$

with $\lambda = nl^2$ the mean number of the particles per collision cell. The molecular chaos assumption has been used for the calculation of the viscosities and thermal conductivities. To analytically obtain the thermal conductivities in Eqs. (6e)-(6h), a large density limit ($\lambda \gg 1$) is employed. We point out that the collisional odd thermal conductivity in Eq. (6h) does not result from a theoretical derivation but is an empirical speculation, since the molecular chaos approximation would predict a vanishing κ_o^{col} .

Combining Eqs. (3)-(5), the conservation equations of the mass, momentum and energy can be written in a concise form,

$$\begin{aligned} \frac{d\rho}{dt} + \rho \nabla \cdot \mathbf{u} &= 0, \\ \rho \frac{d\mathbf{u}}{dt} &= -\nabla p + \hat{\eta} \nabla^2 \mathbf{u} + \hat{\eta}_o \boldsymbol{\varepsilon} \cdot \nabla^2 \mathbf{u}, \\ nk_B \frac{dT}{dt} &= \boldsymbol{\sigma} : \nabla \mathbf{u} + \kappa \nabla^2 T, \end{aligned} \quad (7)$$

where $\hat{\eta} = \eta^{kin} + \eta^{col}$ and $\hat{\eta}_o = \eta_o^{kin} + \eta_o^{col}$. It should be emphasized that the additional unidirectional rotation (i.e., θ) does not produce a net torque on the fluid. Consequently, the anti-symmetric hydrostatic stress is lacking in the odd CSR fluid, which is different from active spinner fluids that are powered by nonzero torque and have nonvanishing anti-symmetric stress even in a quiescent situation [12, 13, 40].

Besides the viscosities and thermal conductivities, the self-diffusion coefficients of the CSR fluid particles are also derived through the same route. Herein, some fluid par-

ticles are tagged, such that the CSR fluid is regarded as a mixture composed of two types of particles (say A and B) with their respective density fields $\rho_A(\mathbf{r}, t)$ and $\rho_B(\mathbf{r}, t)$. The evolution of the density fields is governed by the isothermal self-diffusion equation,

$$\partial_t \Delta \rho = \partial_\alpha D_{\alpha\beta} \partial_\beta \Delta \rho, \quad (8)$$

with $\Delta \rho = \rho_A - \rho_B$ and $D_{\alpha\beta} = D \delta_{\alpha\beta} + D_o \varepsilon_{\alpha\beta}$ being the self-diffusion tensor. Based on the diffusive particle flux obtained through the kinetic theory, the normal self-diffusion coefficient, D , and the odd self-diffusion coefficient, D_o , separately read,

$$\begin{aligned} D &= \frac{k_B T \Delta t}{2m} \frac{2\lambda (1 - \cos \omega \cos \theta)}{(\lambda - 1 + e^{-\lambda}) (1 - 2 \cos \omega \cos \theta + \cos^2 \omega)} \\ &\quad - \frac{k_B T \Delta t}{2m}, \\ D_o &= - \frac{\lambda k_B T \Delta t \cos \omega \sin \theta}{m (\lambda - 1 + e^{-\lambda}) (1 - 2 \cos \omega \cos \theta + \cos^2 \omega)}. \end{aligned} \quad (9)$$

Now, we perform simulations to confirm the existence of odd transport coefficients in the CSR fluid and to verify the validity of the analytical expressions in Eqs. (6) and (9) (see Supplementary Material [39] for the simulation details). In simulations, a boundary-driven shear flow, thermal gradient or concentration gradient is applied to the CSR fluid, and the resulting steady-state stress, heat flux or particle flux is respectively measured. Thus, the corresponding transport coefficients are accurately quantified, as plotted in Fig. 2 that shows the presence of considerable odd transport coefficients. Remarkably, the theoretical predictions based on the microscopic

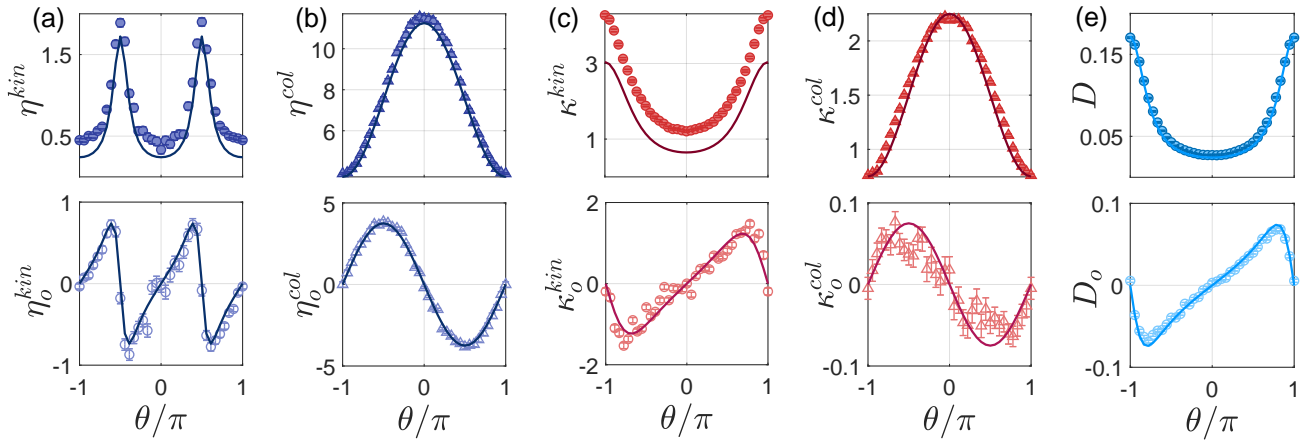


FIG. 2. Viscosities (a,b), thermal conductivities (c,d) and self-diffusion coefficients (e) of the CSRD fluid as a function of the additional rotation angle θ . The solid lines correspond to the theoretical results calculated from Eqs. (6) and Eqs. (9), and the symbols to the simulation measurements. Parameters in (a)-(e): $\omega = 2\pi/3$, $\Delta t = 0.1$, $k_B T = 1$, and $\lambda = 10$.

kinetic theory are in good agreement with the simulation measurements (Fig. 2).

Case studies.—To demonstrate the effects of the odd transport coefficients on the transportation in fluids, three typical transport phenomena are investigated by using both simulation and hydrodynamic theory (see Supplementary Material [39] for the details).

The first example considers a fluid flowing through a channel with stick boundary walls, as sketched in Fig. 3(a). In this situation, the fluid is driven by a constant external force \mathbf{g} and its temperature remains fixed by scaling the thermal energy of the particles. The simulations reveal that both common fluid ($\theta = 0$) and odd fluid exhibit a Poiseuille flow profile (Fig. 3(a)). While, unlike the common fluid, the density distribution of the odd fluid is inhomogeneous across the channel and depends on the odd viscosity of the fluid (Fig. 3(b)).

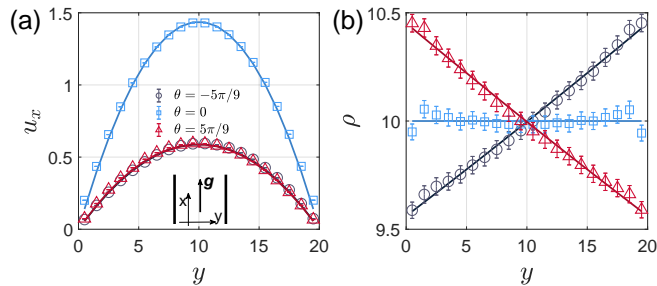


FIG. 3. (a) Velocity profile of the fluid flowing through a channel composed of two nonslip walls, and (b) the corresponding density distribution across the channel. The symbols and lines, respectively, denote the results from the CSRD simulations and hydrodynamic theory where the transport coefficients in Eq. (6) are used. Different symbols represent different $\theta \in (-5\pi/9, 0, 5\pi/9)$. System parameters: $\omega = 2\pi/3$, $\Delta t = 0.5$, $k_B T = 1$, $\rho_0 = 10$, $g = 0.01$, and $L = 20$.

This finding is completely consistent with our previous work on active spinner fluid [12], where the odd viscosity has been proven to cause a transverse Hall-like mass transport under a nonuniform shear. Theoretically, combining Eqs. (7) with the steady-state boundary conditions $u_y = 0$ and $u_x(y)|_{y=0,L} = 0$, the solutions of density and velocity field are given by $\rho = \rho_0$, $u_x = \frac{\rho_0 g}{2\eta} y(L-y)$ for $\hat{\eta}_o = 0$ and $\rho = \frac{\gamma \rho_0 L}{(e^{\gamma L} - 1)} e^{\gamma y}$, $u_x = \frac{g \rho_0 L}{\gamma(1 - e^{\gamma L})\hat{\eta}} [e^{\gamma y} - 1 - (e^{\gamma L} - 1) \frac{y}{L}]$ for nonzero $\hat{\eta}_o$. Here, ρ_0 denotes the mean mass density, L represents the channel width, $g = |\mathbf{g}|$ and $\gamma = \frac{\hat{\eta}_o m g}{\hat{\eta} k_B T}$. The theoretical calculations from the hydrodynamic equations perfectly reproduce the simulation results, as shown in Fig. 3.

The other two examples are steady-state heat conduction and self-diffusion of the odd fluid in a rectangular box of dimensions $L_x \times L_y$. Zero-flux boundary conditions are applied to the left and right walls of the box, while the temperatures (or the tagged-particle concentrations ρ_A) at the bottom and top boundaries are fixed to different values for the case of heat conduction (or self-diffusion). The simulations show that the temperature and concentration distributions of the odd fluid noticeably differ from the common fluid, as presented in Fig. 4. Particularly, in contrast to the common fluids, the isotherms/isoconcentration lines of the odd fluids are not parallel to the isothermal/isoconcentration boundary (namely, the temperature or concentration is not uniform in the x direction). This behavior originates from the transverse heat or particle flux, respectively, induced by the odd thermal conductivity or self-diffusion coefficient. On the other hand, the continuum theory based on Eqs. (7)-(8) indicates that the steady-state temperature and concentration fields both obey the Laplace equation, $\nabla^2 \phi = 0$, with $\phi = T$ for the heat conduction and $\phi = \rho_A$ for the self-diffusion. With the zero-flux boundaries $(\kappa \partial_x T + \kappa_o \partial_y T)|_{x=0,L_x} = 0$ or

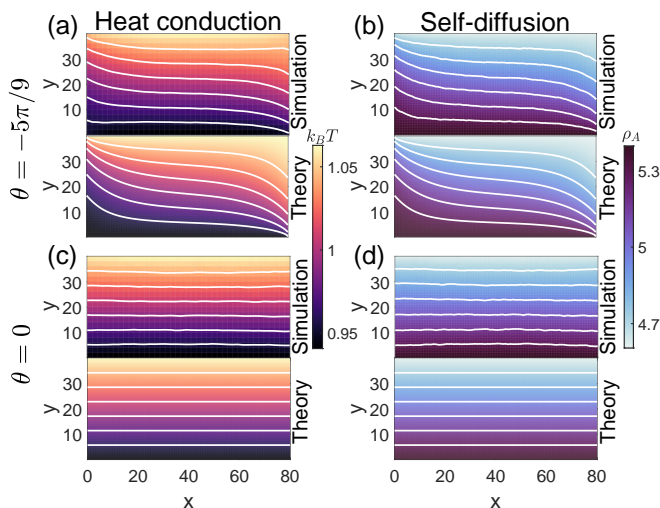


FIG. 4. Heat conduction of the odd fluid (a) and common fluid (c) in a confined box, with $k_B T|_{y=0} = 0.94$ and $k_B T|_{y=L_y} = 1.06$ imposed; self-diffusion of the odd fluid (b) and common fluid (d), with $\rho_A|_{y=0} = 5.4$ and $\rho_A|_{y=L_y} = 4.6$. Here, the color maps represent the temperature or concentration distribution, and the white lines are the isotherms or isoconcentration lines. For comparison, both simulation and theoretical results are given. System parameters: $\Delta t = 0.1$, $\lambda = 10$, $\omega = 5\pi/6$ for (a,c), $\omega = 2\pi/3$ for (b,d), and $\theta = -5\pi/9$ for the odd fluid.

$(D\partial_x\rho_A + D_o\partial_y\rho_A)|_{x=0,L_x} = 0$, and the condition that the values of $\phi|_{y=0,L_y}$ keep fixed, the Laplace equation is solved numerically. The obtained theoretical results compare well to the simulations (Fig. 4), with a relative deviation below %2, highlighting the validity of the CSRD approach in describing the nonequilibrium transport behavior of odd fluids.

Conclusion.—We develop an efficient mesoscale simulation approach for odd fluids (CSRD) by slightly modifying the well-known SRD method that has been extensively used to study complex fluids. The CSRD fluid not only exhibits all odd transport coefficients but also properly captures hydrodynamics, thermal conduction and mass diffusion of real fluids. Furthermore, by a microscopic kinetic theory, we analytically derive the transport coefficients and continuum equations for the CSRD fluid, which precisely describe the transport of the mesoscopic odd fluid. Our work thus paves the way for simulating odd complex fluids at large scales and exploring their unique characteristics.

ACKNOWLEDGMENT

This work was supported by the National Natural Science Foundation of China (No. T2325027, No. 12274448), National Key R&D Program of China (2022YFF0503504).

* jiaoyuxing22@mails.ucas.ac.cn

† mcyang@iphy.ac.cn

- [1] P. M. S. R. De Groot, *Non-Equilibrium Thermodynamics* (Dover Publications, 2011), ISBN 9780486647418.
- [2] J. E. Avron, R. Seiler, and P. G. Zograf, *Phys. Rev. Lett.* **75**, 697 (1995).
- [3] C. Hoyos and D. T. Son, *Phys. Rev. Lett.* **108**, 066805 (2012).
- [4] A. I. Berdyugin, S. G. Xu, F. M. D. Pellegrino, R. K. Kumar, A. Principi, I. Torre, M. B. Shalom, T. Taniguchi, K. Watanabe, I. V. Grigorieva, et al., *Science* **364**, 162 (2019).
- [5] T. Holder, R. Queiroz, and A. Stern, *Phys. Rev. Lett.* **123**, 106801 (2019).
- [6] H. Hulsman, E. Van Waasdjik, A. Burgmans, H. Knaap, and J. Beenakker, *Physica* **50**, 53 (1970), ISSN 0031-8914.
- [7] J. Korving, H. Hulsman, H. F. P. Knaap, and J. J. M. Beenakker, *Physics Letters* **21**, 5 (1966).
- [8] S. Bonella, A. Coretti, L. Rondoni, and G. Ciccotti, *Phys. Rev. E* **96**, 012160 (2017).
- [9] I. Abdoli, E. Kalz, H. D. Vuijk, R. Wittmann, J.-U. Sommer, J. M. Brader, and A. Sharma, *New Journal of Physics* **22**, 093057 (2020).
- [10] E. Kalz, H. D. Vuijk, I. Abdoli, J.-U. Sommer, H. Löwen, and A. Sharma, *Phys. Rev. Lett.* **129**, 090601 (2022).
- [11] V. Soni, E. S. Bililign, S. Magkiriadou, S. Sacanna, D. Bartolo, M. J. Shelley, and W. T. M. Irvine, *Nature Physics* **15**, 1188 (2019).
- [12] X. Lou, Q. Yang, Y. Ding, P. Liu, K. Chen, X. Zhou, F. Ye, R. Podgornik, and M. Yang, *Proceedings of the National Academy of Sciences* **119**, e2201279119 (2022).
- [13] M. Han, M. Fruchart, C. Scheibner, S. Vaikuntanathan, J. J. de Pablo, and V. Vitelli, *Nature Physics* **17**, 1260 (2021).
- [14] D. Banerjee, A. Souslov, A. G. Abanov, and V. Vitelli, *Nature Communications* **8**, 1573 (2017).
- [15] M. Fruchart, M. Han, C. Scheibner, and V. Vitelli, arXiv:2202.02037 (2020).
- [16] T. Markovich and T. C. Lubensky, *Phys. Rev. Lett.* **127**, 048001 (2021).
- [17] C. Hargus, J. M. Epstein, and K. K. Mandadapu, *Phys. Rev. Lett.* **127**, 178001 (2021).
- [18] F. Vega Reyes, M. A. López-Castaño, and Á. Rodríguez-Rivas, *Communications Physics* **5**, 256 (2022).
- [19] Q. Yang, H. Zhu, P. Liu, R. Liu, Q. Shi, K. Chen, N. Zheng, F. Ye, and M. Yang, *Phys. Rev. Lett.* **126**, 198001 (2021).
- [20] A. Souslov, K. Dasbiswas, M. Fruchart, S. Vaikuntanathan, and V. Vitelli, *Phys. Rev. Lett.* **122**, 128001 (2019).
- [21] A. R. Poggioli and D. T. Limmer, *Phys. Rev. Lett.* **130**, 158201 (2023).
- [22] X. M. de Wit, M. Fruchart, T. Khain, F. Toschi, and V. Vitelli, *Nature* **627**, 515 (2024).
- [23] Y. Ding, B. Wang, Q. Yang, Z. Zhao, S. Komura, R. Seto, M. Yang, and F. Ye, *Research* **7**, 0356 (2024).
- [24] C. J. O. Reichhardt and C. Reichhardt, *Europhysics Letters* **137**, 66004 (2022).
- [25] Y. Hosaka, S. Komura, and D. Andelman, *Phys. Rev. E* **103**, 042610 (2021).

- [26] Q. Yang, H. Liang, R. Liu, K. Chen, F. Ye, and M. Yang, *Chinese Physics Letters* **38**, 128701 (2021).
- [27] S. Succi, *The Lattice Boltzmann Equation for Fluid Dynamics and Beyond* (Oxford University Press, 2001), ISBN 9780198503989.
- [28] A. J. C. Ladd, *Journal of Fluid Mechanics* **271**, 285–309 (1994).
- [29] A. J. C. Ladd, *Journal of Fluid Mechanics* **271**, 311–339 (1994).
- [30] P. Español and P. Warren, *Europhysics Letters* **30**, 191 (1995).
- [31] P. J. Hoogerbrugge and J. M. V. A. Koelman, *Europhysics Letters* **19**, 155 (1992).
- [32] A. Malevanets and R. Kapral, *The Journal of Chemical Physics* **110**, 8605 (1999), ISSN 0021-9606.
- [33] A. Malevanets and R. Kapral, *The Journal of Chemical Physics* **112**, 7260 (2000), ISSN 0021-9606.
- [34] J. T. Padding and A. A. Louis, *Phys. Rev. E* **74**, 031402 (2006).
- [35] R. Kapral, *Adv. Chem. Phys.* **140**, 89 (2008).
- [36] G. Gompper, T. Ihle, D. M. Kroll, and R. G. Winkler, *Adv. Polym. Sci.* **221**, 1 (2009).
- [37] T. Ihle and D. M. Kroll, *Phys. Rev. E* **63**, 020201 (2001).
- [38] C. M. Pooley and J. M. Yeomans, *J. Phys. Chem. B* **109**, 6505 (2005).
- [39] See Supplemental Material at XXX for details of derivation and simulations, which includes Refs. [41,42].
- [40] J.-C. Tsai, F. Ye, J. Rodriguez, J. P. Gollub, and T. C. Lubensky, *Phys. Rev. Lett.* **94**, 214301 (2005).
- [41] F. Müller-Plathe, *Phys. Rev. E* **59**, 4894 (1999).
- [42] F. Müller-Plathe and P. Bordat, *Reverse Non-equilibrium Molecular Dynamics* (Springer Berlin Heidelberg, Berlin, Heidelberg, 2004), pp. 310–326.